Available online on 15.05.2019 at http://jddtonline.info

Journal of Drug Delivery and Therapeutics

Open Access to Pharmaceutical and Medical Research

Open Access Research Article

Optimization and Characterization Ezogabine-Loaded Nanosuspension for Enhancement of Bioavailability by "Bottom-Up" Technology Using 3^2 Factorial Design

S Revathi*, MD Dhanaraju

GIET School of Pharmacy, Rajahmundry, Andhra Pradesh, India

ABSTRACT

Ezogabine, an antiepileptic drug used for treating partial epilepsies. It is poorly soluble in water. The dose ranges from 50 mg to 400 mg and the oral bioavailability is 60%. The aim of this research work was to formulate and characterize nanosuspensions of ezogabine with an intention to enhance the oral bioavailability using 3^2 factorial design. Nanosuspensions were prepared by the "bottom-up" nanoprecipitation method using 3^2 factorial design and evaluation for particle size, saturation solubility, zeta potential, entrapment efficiency, and in-vitro drug release was done. The FTIR was used to confirm compatibility and to rule out any possible interactions between drug and carriers. The optimal nanosuspension was obtained with particle size of 510.4 nm, saturation solubility of 557 µg/ml, zeta potential of - 4.49 mV, entrapment efficiency of 96.82%, and in-vitro drug release of 100.14%. Also, the optimal formulation was found to be stable in the accelerated conditions. Data of nanosuspensions were fit in to different equations and kinetic models and found to exhibit first order release kinetics with class II transport mechanism of diffusion. The scanning electron microscopy studies showed elongated nanoparticles with porous surface. The "Bottom up" method can be successfully employed to produce ezogabine nanosuspensions achieving reduced particle size and enhancing dissolution rate by increasing the saturation solubility and remained stable at 25 °C.

Keywords: Nanosuspension, saturation solubility, bottom up.

Article Info: Received 22 March 2019; Review Completed 04 May 2019; Accepted 06 May 2019; Available online 15 May 2019

Cite this article as:

Revathi S, Dhanaraju MD, Optimization and Characterization Ezogabine-Loaded Nanosuspension for Enhancement of Bioavailability by "Bottom-Up" Technology Using 3^2 Factorial Design, Journal of Drug Delivery and Therapeutics. 2019; 9(3):227-237 **http://dx.doi.org/10.22270/jddt.v9i3.2860**

***Address for Correspondence:**

S Revathi, GIET School of Pharmacy, Rajahmundry, Andhra Pradesh, India

INTRODUCTION

Among the total populace, the most predominant of the unfeigned neurological unhinge is epilepsy which is most feigning about 0.5 to 1%. A seizure is a clinical denotation, ensuing about because of a remit sequence of unnatural extravagant or synchronous neuronal movement in the brain. Epilepsy is a brain unhinge described by an inveterate sensitivity to create epileptic seizures with optional neurobiological, intellectual, mental, and social outcomes.

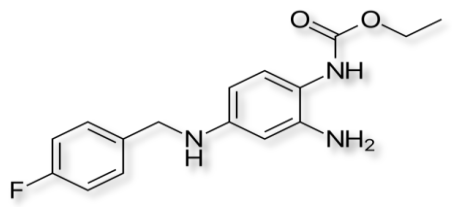

Fig. 1: Chemical structure of Ezogabine

Patients with epilepsy are at an expanded danger of untimely demise with a mortality danger of 1.2 to 9.3 of all reasons for demise and a 24% long term casualty rate. [1, 2]

Ezogabine deeds as a neuronal KCNQ/Kv7 potassium channel opener. It is an antiepileptic drug practised for the intervention of partial epilepsies. Its primary mechanism of action as a positive allosteric modulator of KCNQ2-5 ion channels defines ezogabine as the first neuronal potassium channel opener for the treatment of epilepsy. KCNQ2-5 channels are predominantly expressed in neurons and are important determinants of cellular excitability, as indicated by the occurrence of human genetic mutations in KCNQ channels that underlie inheritable disorders including, in the case of KCNQ2/3, the syndrome of benign familial neonatal convulsions. At present commercialized potassium channel opener is established completely in oral dosage frame. Be that as it may, elective and specifically, intranasal route may give more benefits when compared to oral route. The fallouts of oral route of potassium channel opener admits gastrointestinal disorderlinesses, urinary perturbs etc. [3] Intranasal route conveyance is debated as a feasible and captivating route for versatile drugs. [4]

Common methodology for solvability melioration is micronization of medication. The process of micronization expands the dissolution rate the medication because of surface area expansion however it does not alter the

saturation solvability. [5] Another significant perspective is the expansion in saturation solvability. Additionally, as per Kelvin and Ostwald-Freundlich comparison, the saturation solvency can be enhanced because of the exaggerated dissolution coerce. [6]

This submicron colloidal molecule dispersion of drug which are stabilized by surfactant or concoction of surfactants is called as nanosuspensions. Nanosuspensions are discerned from nanoparticles which are polymeric colloidal carriers of medication, and from solid lipid nanocarriers, which are lipidic carriers of medication. [5]

Nanosuspension is a carrier - free colloidal dosage form which comprises basically of arrant drug nanoparticles and it needs minimal measure of surfactant to stabilize them. [7]

The restriction of this precipitation method is that the medication should be dissolvable in no less than one solvent and this solvent should be miscible with antisolvent. Nanosuspensions are colloidal dispersions and biphasic framework comprising of medication scattered in an aqueous medium in which the width of the suspended particles is under 1 μm in size. In bottom up method, the nanoprecipitation strategy confronts several benefits being quick and simple to accomplish. [8]

The bottom up technique is employed to formulate the nanosuspension on account of various merits such as eminent drug entrapment efficiency for poorly dissolvable drugs, constringe particle size distribution, extravagant batch-to-batch reproducibility, no necessity of homogenization, simple method of preparation, comfort of scale up and economical instruments mandatory. [9]

Generally used electrostatic stabilizers are polysorbates and sodium lauryl sulphate. Steric stabilizers which are normally used are hydroxypropyl methylcellulose, hydroxypropyl cellulose, polyvinylpyrrolidone, and poloxamer. [6]

The aim and objective of this study was to formulate ezogabine nanosuspension by bottom-up technique applying 3^2 factorial design and modifying to enhance the saturation solubility, entrapment efficiency & dissolution rate, reduce the particle size, and to check stability of ezogabine. The three level designs are useful for investigating quadratic effects between the response and each of the factors. Urea and surfactant concentration are used as independent factors. The optimized nanosuspension formulation was assessed through assorted in-vitro parameters.

MATERIALS USED

Ezogabine was received as gift sample from Lupin Pharma, Maharashtra, India. Urea is obtained as a gift sample from Spectrum labs, Hyderabad. All other chemicals and solvents used are from Yarrow Chem Products, Mumbai.

METHODOLOGY

Preformulation Studies

Compatibility Studies

IR spectroscopy can be used to investigate and predict any physicochemical interactions between different components in a formulation and therefore it can be used for the selection of compatible excipient.

Compatibility of the drug (ezogabine) with excipient (urea) used to produce nanosuspension was established by Infrared absorption spectral analysis. I.R spectral analysis of pure ezogabine and urea was carried out. This study was carried out to detect any changes in chemical constitution of drug after combining it with the excipient.

One part of the sample and three parts of potassium bromide were taken in a mortar and triturated. A small amount of triturated sample was taken into pellet maker and was compressed at 10 kg/cm2 using hydraulic press. The pellet was kept onto the sample holder and scanned from 4000 cn-1 to 400 cm-1 using Perkin-Elmer spectrum RX1 FT-IR spectrometer model. I.R spectra was compared and checked for any shifting in functional groups or peaks. [10]

Solubility studies of ezogabine

Solubility of ezogabine in different solvents such as water, acetone, ethanol, and dimethyl sulfoxide was determined by shake flask method. An excess amount of ezogabine was added to each volumetric flask containing the selected vehicle and mixed thoroughly. The volumetric flasks were then fixed onto a water bath shaker and shaken for 24 hr at 25 °C. Samples were removed after a specified time and filtered through 0.22 µm syringe driven membrane filter unit. The filtrates were then analyzed by ultraviolet (UV) spectrophotometer at 218 nm to evaluate the amount of drug dissolved. [4, 11]

Method of preparation of nanoprecipitation by "Bottom up" Technique

The nanosuspension was obtained by the precipitation process of "Bottom up" technique. The 100 mg of drug (ezogabine) was initially dissolved in 10 ml of polar solvent (ethanol) to devise the organic phase. The coded amount of carrier (urea) and the surfactant (sodium lauryl sulphate) were added to 30 ml of distilled water (antisolvent) to devise the aqueous phase. The organic phase was then slowly added drop wise using syringe into the aqueous phase which is kept at room temperature and stirred with a speed of 900-1000 rpm for 1 hr using magnetic stirrer. Then, the solution is homogenized for next 1 hour to remove excess of ethanol. [12, 13, 21]

3^2 Full Factorial Design

A 3^2 full factorial design was applied to examine the effect of independent variables carrier (urea X1) and surfactant concentration (sodium lauryl sulphate X2) as in Table 1 on dependent variables such as particle size (Y1), saturation solubility (Y2), zeta potential (Y3), entrapment efficiency (Y4), and *in-vitro* drug release (Y5). [14] The graphs and mathematical models were computed using MINITAB ® 17.1.0 (UK) software. [23]

Table 1: Coded independent variables

Coded Level	-1	0	+1
X1: Carrier Concentration (mg) – Urea	10	15	20
X2: Surfactant Concentration (mg) - SLS	1	2	3

Evaluation Characteristics of Nanosuspension

Scanning Electron Microscopy

Scanning Electron Microscopy has been used to determine particle size distribution, surface topography, texture and to examine the morphology of fractured surface. Surface morphology of the specimens was determined by using a scanning electron microscope, Model JSM 84 0A, JEOI, Japan. The samples are dried thoroughly in vacuum desiccator before mounting on brass specimen studies, using double sided adhesive tape. Gold-palladium alloy of 120 °A Knees was coated on the sample sputter coating unit (Model E5 100 Polaron U.K) in Argon at ambient of 8-10 with plasma voltage about 20mA. The sputtering was done for nearly 5 minutes to obtain uniform coating on the sample to enable good quality SEM images. The SEM was operated at low

accelerating voltage of about 15KV with load current about 80mA. The objective lens aperture has a diameter of 240 microns and working distance WD=39mm. [4]

Polydispersity Index

Polydispersity Index is an index of width or spread or variation within the particle size distribution. Monodisperse samples have a lower PDI value, whereas higher value of PDI indicates a wider particle size distribution and the polydisperse nature of the sample. [15] PDI is calculated by the using following formula:

$$PDI = \Delta d/davg$$

where, Δd is the width of distribution and davg is the average particle size. The usual range of PDI values is as follows,

Table 2: Polydispersity Index of nanoparticles

Polydispersity Index	Type of dispersion
0 – 0.05	Monodisperse standard
0.05 – 0.08	Nearly monodisperse
0.08 – 0.7	Midrange polydispersity
> 0.7	Very polydisperse

Saturation solubility studies

Saturation solubility measurements were assayed through ultraviolet absorbance determination at 218 nm using UV-Visible spectrophotometer (SL 210 Elico). The process was carried out for both the unprocessed pure drug and different batches of nanosuspensions. Nanosuspension equivalent to 100 mg of ezogabine were taken and individually hosted into stoppered conical flask having 10 ml of distilled water. The flasks were closed and retained in thermostatically controlled mechanical orbital shaking incubator (CIS-24 BL, REMI) for 48 hrs at 37 °C and equilibrated. The samples were collected after the specified time interval, filtered, diluted with distilled water suitably and analyzed. [5, 16]

Zeta potential analysis

Zeta potential of the suspension is measured by Malvern Zetasizer using the Helmholtz-Smoluchowski equation. The Zetasizer mainly consists of laser which is used to provide a light source to illuminate the particles within the sample. For zeta potential measurements this light splits to provide an incident and reference beam. The incident laser beam passes through the centre of the sample cell and the scattered light at an angle of about 130 is detected. Zetasizer software produces a frequency spectrum from which the electrophoretic mobility occurs. Hence the zeta potential is calculated and stability is checked by comparing with the Table 3. [4]

Table 3: Zeta potential for suspensions/emulsions and their stability

Zeta potential (mv)	Stability behaviour
From 0 to ± 5	Rapid coagulation or flocculation
From ± 10 to ± 30	Incipient stability
From ± 30 to ± 40	Moderate stability
From ± 40 to ± 50	Good stability
More than ± 61	Excellent stability

Percentage Entrapment efficiency

The formulated nanosuspensions were centrifuged using cooling ultracentrifuge at 5 °C temperature and 25,000 rpm for 30 min. The amount of free drug was measured by taking the absorbance by diluting the supernatant solution using UV spectrophotometer against blank/control nanosuspensions. The experimentation was executed thrice for each batch and the mean was calculated. [17]

$$\%\ Entrapment\ Efficiency = \frac{(Total\ amount\ of\ drug - Free\ dissoved\ drug)\ \ X\ 100}{Total\ amount\ of\ drug}$$

In-vitro drug release studies

In-vitro drug release studies were performed in USP apparatus Type II (TDT -08L, Electrolab) using paddle method at rotation speed of 50 rpm. Dissolution was carried out in pH 6.8 buffer as dissolution medium. The volume and temperature of the dissolution medium were 900 ml and 37.0 ± 0.5°C respectively. Samples (5 ml) were withdrawn periodically at 5, 10, 15, 20 min and replaced with an equal volume of fresh pH 6.8. Samples were suitably diluted and filtered through a filter paper (0.22 µm, Whatman Inc., USA). The filtrate was then subject to the UV analysis against the blank (pH 6.8). Percentage cumulative drug release was calculated based on the standard UV calibration curve at 218 nm. [4]

Kinetics of Drug Release

In order to analyze the drug release mechanism, in vitro release data were fitted into a zero-order, first order, Higuchi, Hixon-Crowell cube root law, and Korsmeyer-Peppas models as in Table 4. The zero order rate Eq. 1 describes the systems where the drug release rate is independent of its concentration.

$$C = k_o t \quad \ldots\ldots\ldots\ldots (1)$$ Where,

C is the concentration of the drug at time (t) and ko is the zero-order release rate constant.

The first order equation Eq. 2 describes the release from a system where the release rate is concentration dependent.

$$\log C = \log C_0 - kt / 2.303 \quad \ldots\ldots\ldots\ldots (2)$$

Higuchi described the release of drugs from porous, insoluble matrix as a square root of time dependent process based on Fickian diffusion as shown in Eq. 3.

$$Q = K_t^{1/2} \quad \ldots\ldots\ldots\ldots (3)$$

The Hixson-Crowell cube root law Eq. 4 describes the release from systems where there is a change in surface area and diameter of particles.

$$Q_0^{1/3} - Q_t^{1/3} = K_{HC}\, t \quad \ldots\ldots\ldots\ldots \quad (4)$$

To evaluate the mechanism of drug release, data for the first 60% of drug release were plotted into the Korsmeyer et al's Eq. 5 as log cumulative percentage of drug released Vs log time, and the exponent (n) was calculated using the slope of the straight line.

$$M_t / M_\infty = K t^n \quad \ldots\ldots\ldots\ldots \quad (5)$$

where (M_t/M_∞) is the fractional solute release, (t) is the release time, (K) is a kinetic constant characteristic of the drug/polymer system, and (n) is an exponent that characterizes the mechanism of release of tracers .

If the exponent n = 0.45, then the drug release mechanism is Fickian diffusion and if 0.45 < n < 0.89, then it is non-Fickian or anomalous diffusion. [18]

Table 4: Release kinetics models

MODELS	EQUATIONS	GRAPH
Zero order	$Q_t = Q_0 + K_0 t$	% Cumulative release Vs time
First order	$\ln Q_t = \ln Q_t + K_1 t$	Log % cumulative drug remaining Vs time
Higuchi matrix	$Q_t = Q_0 - K_H t_{1/2}$	% Cumulative release Vs √time
Korsmeyer-Peppa's	$\log (Q_t / Q_\infty) = \log K + n \log t$	Log % cumulative release Vs log time
Hixon-Crowell root law	$Q_0^{1/3} - Q_t^{1/3} = K_{HC}\, t$	Time Vs cube root % drug release

Stability Studies

Stability is defined as "The capacity of the drug product to remain within specifications established to ensure its identity, strength, quality and purity" (FDA 1987). Accelerated stability study was conducted to monitor the physical and chemical stability of Retigabine nanosuspension by using stability chamber at room temperature (25 °C and 60% RH) and accelerated conditions (40 °C and 75% RH) for 3 months according to ICH guidelines (Table 5). Assay was used as the stability parameter. At periodic time intervals, the samples were withdrawn and analyzed for drug content. [18, 22]

Table 5: ICH guidelines for stability studies

Types	Storage Conditions		Minimum Time Period (Months)
	Temperature (°C)	Humidity (%)	
Long Term Testing	25 °C ± 2 °C	60% ± 5% RH	12
Intermediate Testing	30 °C ± 2 °C	65% ± 5% RH	6
Accelerated Testing	40 °C ± 2 °C	75% ± 5% RH	3

RESULTS & DISCUSSION

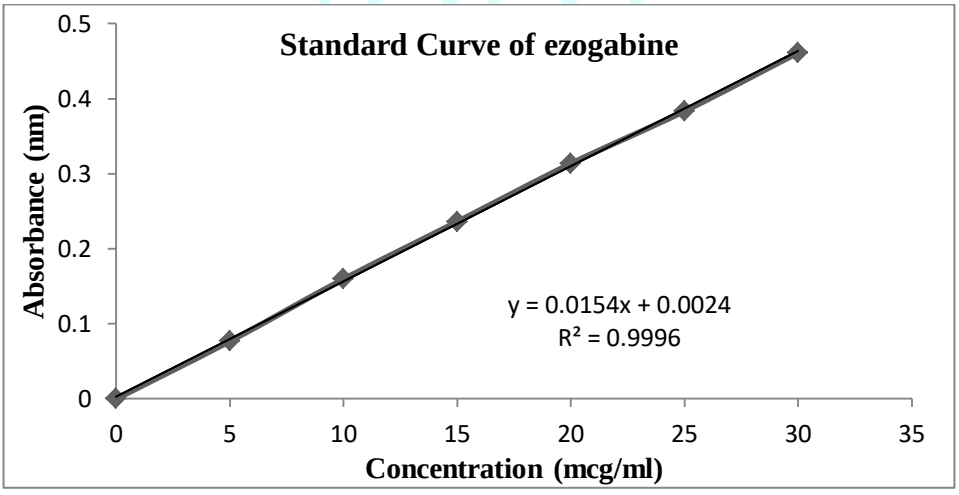

Fig. 2: Standard curve of ezogabine

The linearity was plotted for absorbance (A) against the concentration(C) with R^2 value 0.999 and with the slope equation y=0.015x + 0.002.

FTIR Studies

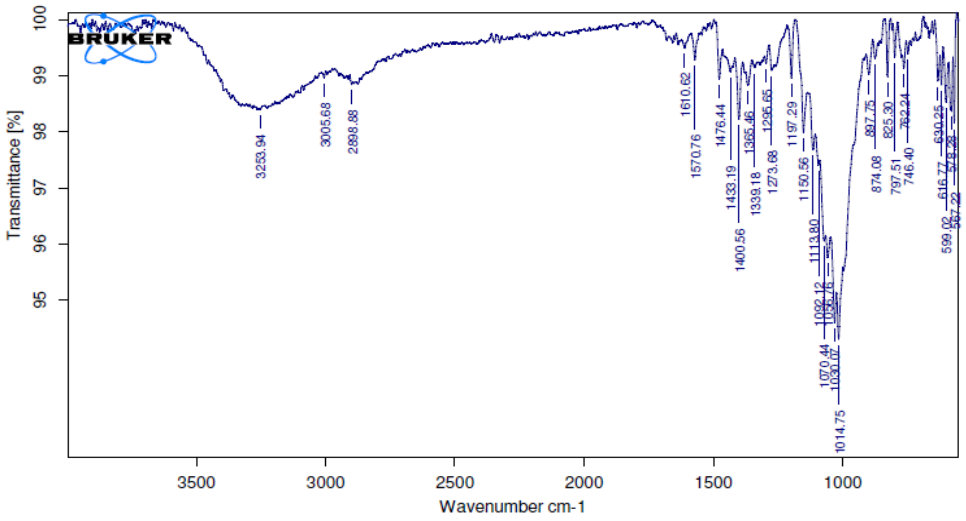

Fig. 3: FTIR of ezogabine

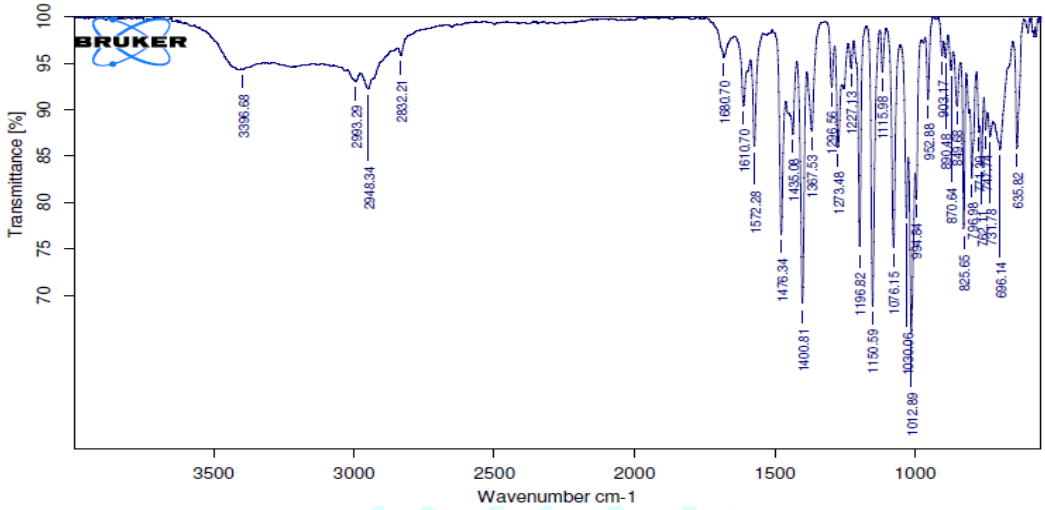

Fig. 4: FTIR of ezogabine with Urea

Table 6: Interpretation of FT-IR spectra of Pure Drug (ezogabine)

S. No	Functional Groups	Assessment Peak of Pure Drug CM^{-1}	Range of Groups CM^{-1}
1	C-H stretching	3253.94	3333-3267
2	C-H stretching	3005	3100-3000
3	C-H stretching	2898	2960-2850
4	N-H Bending	1570	1650-1580
5	C-N Stretching	1014	1340-1020
6	C-H Bending	797	870-675

Table 7: Interpretation of FT-IR spectra of Drug & Urea

S. No	Functional Groups	Assessment Peak of Drug & Urea CM^{-1}	Range of Groups CM^{-1}
1	N-H stretching	3348.48	3500-3300
2	C=O stretching	1703.42	1760-1670
3	C-H stretching	3253.94	3333-3267
4	N-H Bending	1570	1650-1580

Table 8: Solubility profile of ezogabine in various solvents

S. No	Solvent	Solubility (mg/ml)
1	Water	0.02
2	Acetone	25.2
3	DMSO	27.9
4	Ethanol	29.1

Since ezogabine is poorly soluble in water and more soluble in ethanol when compared to other solvents such as acetone and DMSO, it is selected for the solubilising the ezogabine in nanosuspensions. The solubility of ezogabine in ethanol is higher when compared to that of other solvents may be due to polarity character of ethanol.

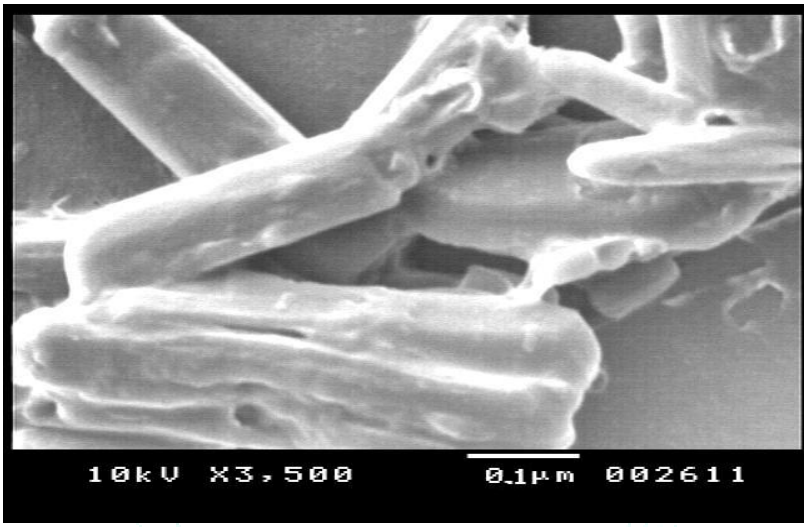

Fig. 5: SEM analysis of F9 at 0.1µm

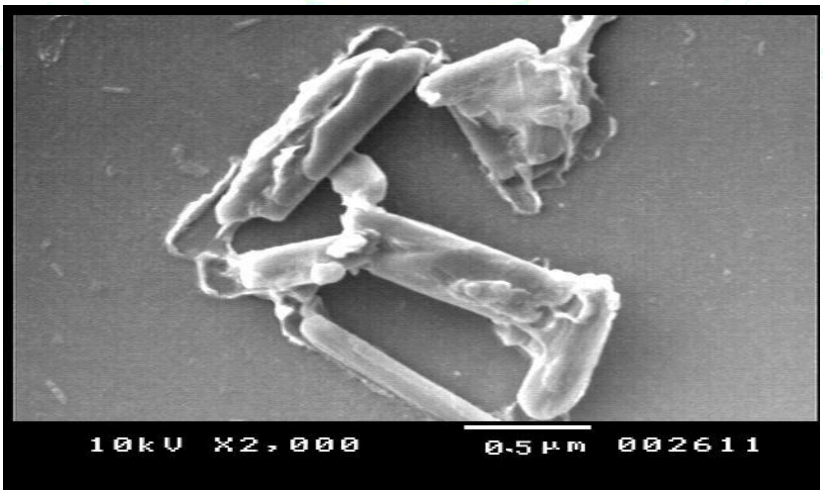

Fig. 6: SEM analysis of F9 at 0.5 µm

The surface studies showed elongated nanoparticles with porous surface.

Table 9: Evaluation characteristics of dependent variables

F. Code	VARIABLES		RESPONSES				
	X1 Urea (mg)	X2 SLS (mg)	Y1 Particle size (nm)	Y2 Saturation Solubility (µg/ml)	Y3 Zeta Potential (mV)	Y4 Entrapment Efficiency (%)	Y5 In-vitro drug release in 20 minutes (%)
F1	-1	-1	582.1	392 ± 0.23	- 3.89	86.96 ± 1.85	94.32 ± 0.23
F2	-1	0	563.5	471 ± 0.58	- 4.21	88.19 ± 0.13	95.63 ± 0.52
F3	-1	1	541.8	528 ± 0.12	- 4.46	90.75 ± 0.32	97.86 ± 0.38
F4	0	-1	597.2	398 ± 0.62	- 3.85	89.31 ± 0.12	97.38 ± 0.14
F5	0	0	574.7	474 ± 0.24	- 4.17	91.76 ± 0.15	98.84 ± 0.27
F6	0	1	551.2	534 ± 0.82	- 4.43	93.81 ± 0.51	99.91 ± 0.36
F7	1	-1	593.3	395 ± 0.51	- 3.87	92.48 ± 0.22	99.07 ± 0.15
F8	1	0	568.6	468 ± 0.35	- 4.23	94.53 ± 0.32	99.82 ± 0.21
F9	1	1	510.4	557 ± 0.77	- 4.49	96.82 ± 0.14	100.14 ± 0.43

All the above values represent mean ± S.D: n = 3

Particle size distribution

The particle size was measured using a Zetasizer Nano ZS (Malvern Instruments, Malvern, UK). The average particle diameter was found to be 582 to 597 nm, 563 nm to 574 nm, and 510 nm to 551 nm for 1 ml, 2 ml and 3 ml of surfactant concentration respectively. The particle size distribution studies showed that the optimized formulation particle size was in the range 510.4 nm. Size reduction of drug particles leads to an enhanced dissolution rate not only because of increased surface area but also because of saturation solubility as described by Freundlich-Ostwald equation. All the formulations having a particle size in the nanometer range and showing ideal surface morphology. [7]

The particle size distribution studies showed that the optimised formulation F9 particle size was in the range 510 nm and whereas unprocessed drug shows 50 – 60 µm in size. All the formulations having a particle size in the nanometre range and showing ideal surface morphology. The particle size of the formulations ranged from 510.4 nm to 597.2 nm. The particle size has been decreased with increase in the surfactant concentration on the formulations irrespective of carrier concentration. The optimized formulation F9 showed a lowest particle size possibly because of highest concentration of surfactant used. The carrier concentration has no significant effect on particle size. The optimized formulation F9 has PDI of 0.251 showing midrange polydispersity indicating that the particles are uniformly distributed.

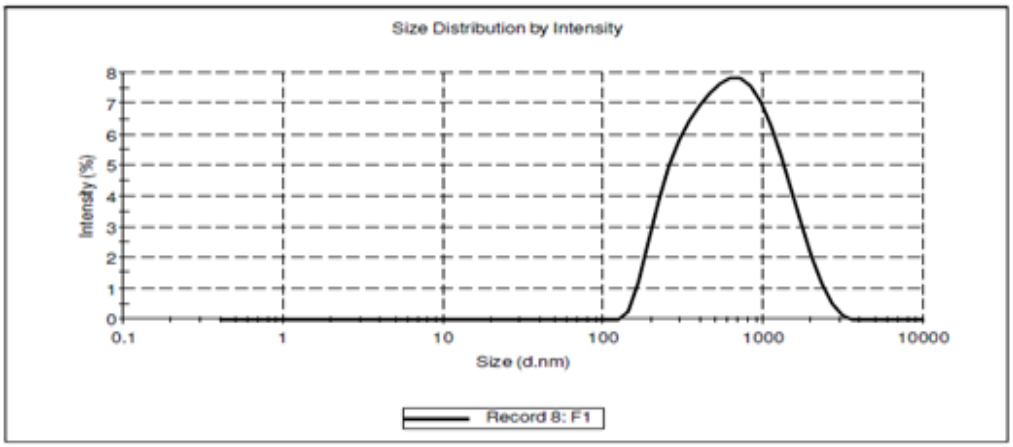

Fig. 7: Particle size and Polydispersity index of F9

Saturation Solubility Studies

The saturation solubility studies indicates that nanosuspensions shows maximum solubility compared to unprocessed drug which is due to the crystalline nature of pure drug. The saturation solubility also showed a major effect with increase in surfactant concentration may be due to the decreasing the interfacial tension between the phases. Approximately three times increase in saturation solubility of prepared nanosuspension was observed than that of unprocessed drug.

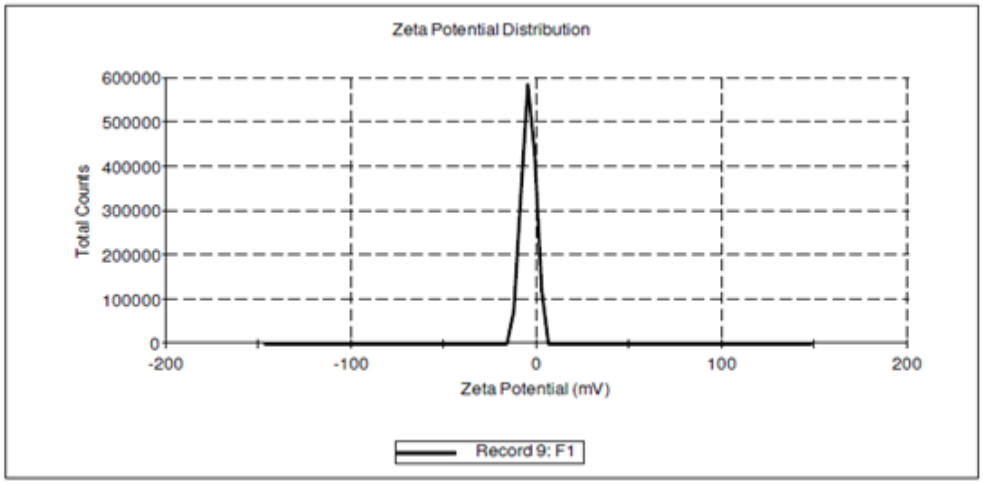

Fig. 8: Zeta potential of F9

Zeta potential is related to the stability of samples. Particles that are small enough with high zeta potential will confer stability resisting aggregation. The zeta potential of the prepared nanosuspension F9 was found to be - 4.49. The values in the range -5 mV to +5 mV indicate fast aggregation/coagulation leading to drug release. [19] The surface charge on particles may arise due to ionisation of particle surface or adsorption of surfactant contributing to stabilisation of the nanosuspension. [20]

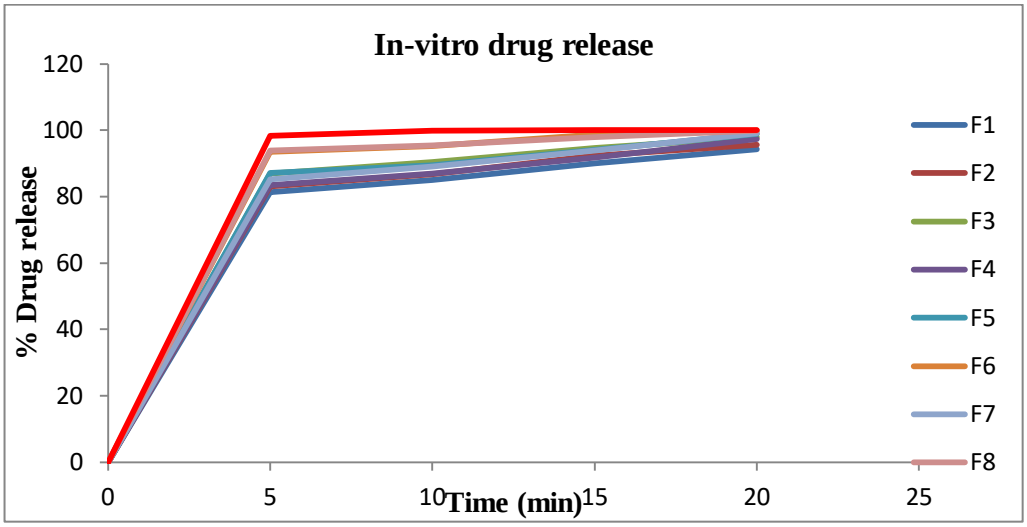

Fig. 9: In-vitro drug release of F1-F9

On comparing the formulations, the F9 showed 100.14% of drug release in 15 minutes, whereas other formulations required 20 minutes to yield complete drug release. This may be due to the increased saturation solubility and decreased particle size of the formulation F9 when compared to that of others. When the data of in-vitro drug release from nanosuspensions were fit in to different equations and kinetic models to explain release kinetics, the best formulation showed first order drug release with anomalous or Class II transport mechanism of drug by diffusion.

Table 10: Kinetic values of F1 - F9

F.code	Zero-order plots	First-order plots	Higuchi's Plots	Korsmeyer et al's plots		Hixon-Crowell	Possible Drug Release mechanism
	(R^2)	(R^2)	(R^2)	(n)	(R^2)	R^2	
F1	0.622	0.870	0.866	1.527	0.830	0.778	First order Class II Transport
F2	0.618	0.887	0.863	1.533	0.830	0.786	First order Class II Transport
F3	0.599	0.907	0.849	1.541	0.849	0.791	First order Class II Transport
F4	0.627	0.913	0.868	1.535	0.831	0.822	First order Class II Transport
F5	0.605	0.914	0.853	1.541	0.827	0.822	First order Class II Transport
F6	0.557	0.937	0.819	1.550	0.819	0.812	First order Class II Transport
F7	0.625	0.926	0.867	1.542	0.831	0.855	First order Class II Transport
F8	0.551	0.909	0.813	1.548	0.818	0.778	First order Class II Transport
F9	0.512	0.600	0.851	1.552	0.812	0.725	First order Class II Transport

Table 11: Stability Studies Data of F9

Storage Condition	0 Days	15 Days	30 Days	45 Days	60 Days	90 Days
25 °C & 60 % RH	100.36 ± 0.45	97.2 ± 0.25	96.4 ± 0.67	94.1 ± 0.52	92.5 ± 0.36	91.7 ± 0.27
Particle size	510.4 nm	-	510.9 nm	-	511.3 nm	511.8 nm
40 °C & 75 % RH	98.4 ± 0.45	94.5 ± 0.75	92.1 ± 0.12	90.1 ± 0.12	86.3 ± 0.36	84.9 ± 0.19
Particle size	510.4 nm	-	519.7 nm	-	528.9 nm	537.2 nm

All the above values represent % mean± S.D: n=3

The formulations at 25 °C remained stable, whereas only those stored at higher temperatures of 40 °C exhibited an increase in mean particle size. The increase in size perhaps may be due to dehydration of the chains and subsequent loss of protection of the nanoparticles. Sedimentation was observed in all the conditions but the preparations were easily redispersed on shaking.

Table 12: Regression coefficients for each term in the regression model

Polynomial Equations	R^2
Y1 = 564.76 - 2.29 X1_10 + 9.61 X1_15 - 7.32 X1_20 + 26.11 X2_1 + 4.18 X2_2 - 30.29 X2_3	**89.16**
Y2 = 468.56 - 4.89 X1_10 + 0.11 X1_15 + 4.78 X1_20 - 73.56 X2_1 + 2.44 X2_2 + 71.11 X2_3	**98.86**
Y3 = 4.17778 + 0.00889 X1_10 - 0.02778 X1_15 + 0.01889 X1_20 - 0.30778 X2_1 + 0.02556 X2_2 + 0.28222 X2_3	**99.84**
Y4 = 91.623 - 2.990 X1_10 + 0.003 X1_15 + 2.987 X1_20 - 2.040 X2_1 - 0.130 X2_2 + 2.170 X2_3	**99.51**
Y5 = 98.108 - 2.171 X1_10 + 0.602 X1_15 + 1.569 X1_20 - 1.184 X2_1 - 0.011 X2_2 + 1.196 X2_3	**98.10**

From the results of ANOVA, it was observed that the independent factor X1 (carrier concentration) influences the dependent factors Y4 (entrapment efficiency) and Y5 (in-vitro diffusion). The independent factor X2 (surfactant concentration) has significant effect the dependent factors Y1 (particle size), Y2 (saturation solubility), Y3 (zeta potential), & Y5 (in-vitro dissolution) and moderate effect on Y4 (entrapment efficiency).

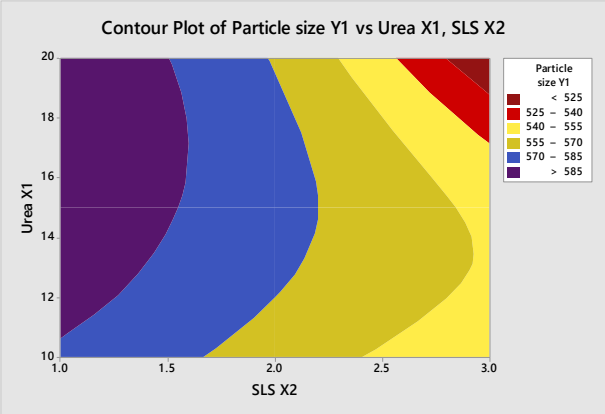

Fig. 10: Contour plot of particle size Vs Urea & SLS

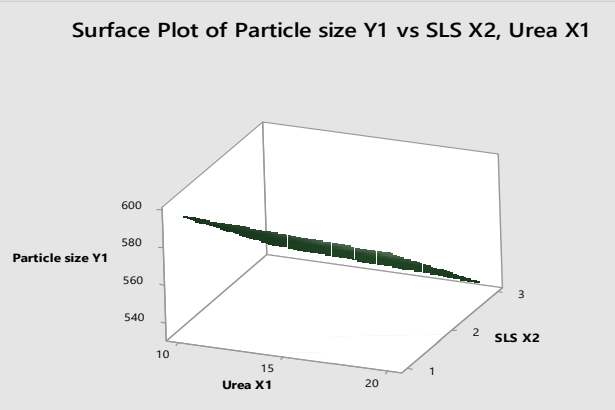

Fig. 11: Surface plot of particle size Vs Urea & SLS

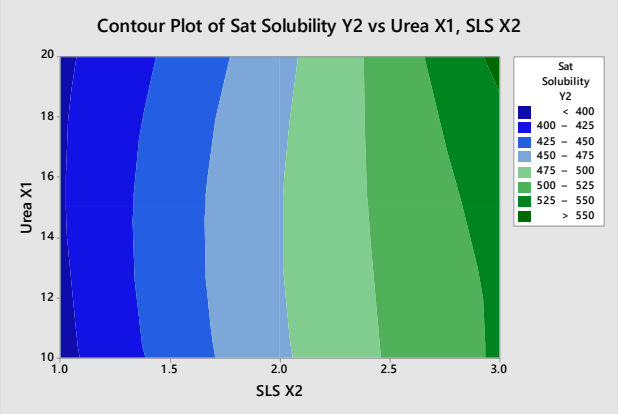

Fig. 12: Contour plot of Saturated Solubility Vs Urea & SLS

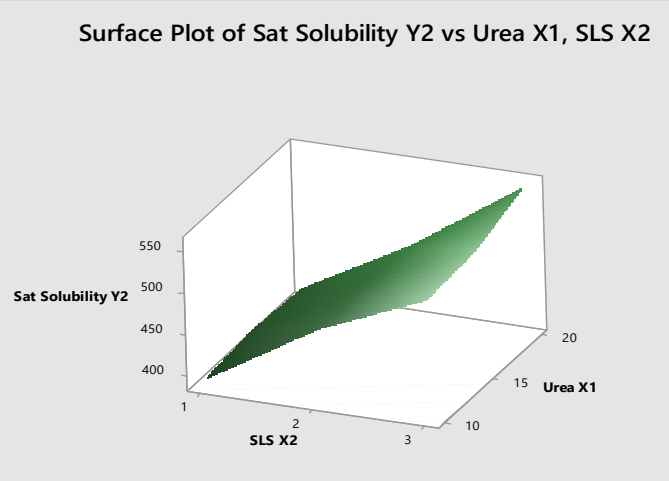

Fig. 13: Surface plot of Saturated Solubility Vs Urea & SLS

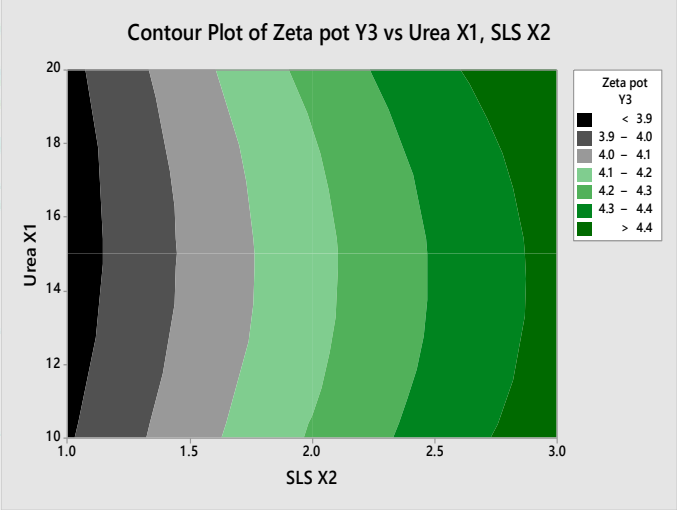

Fig. 14: Contour plot of Zeta potential Vs Urea & SLS

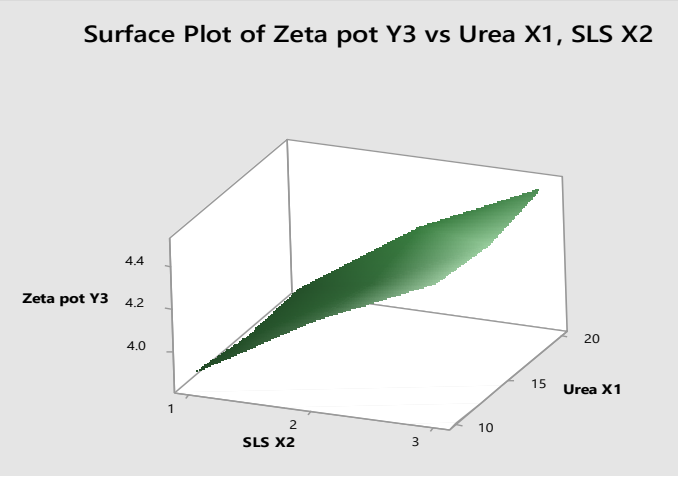

Fig. 15: Surface plot of Zeta potential Vs Urea & SLS

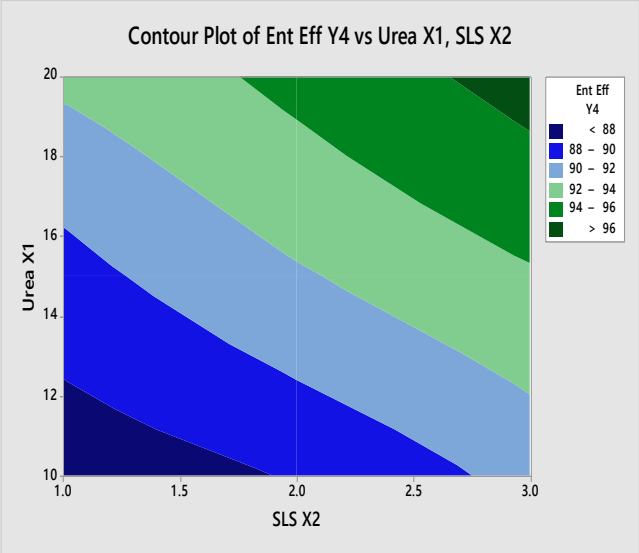

Fig 16: Contour plot of Entrapment Efficiency Vs Urea & SLS

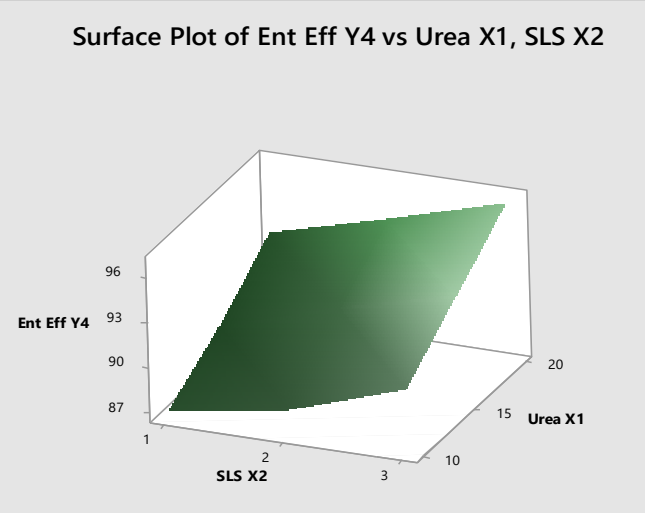

Fig 17: Surface plot of Entrapment Efficiency Vs Urea & SLS

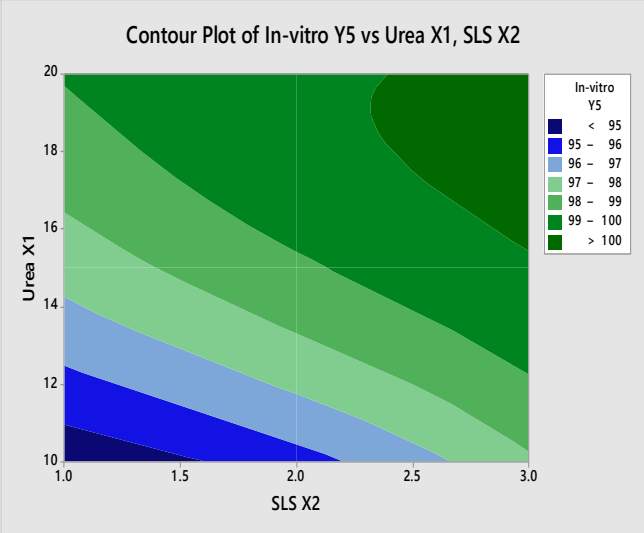

Fig 18: Contour plot of In-vitro dissolution Vs Urea & SLS

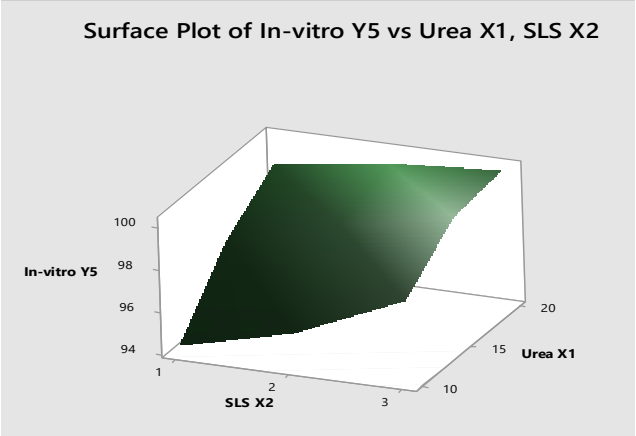

Fig 19: Surface plot of In-vitro dissolution Vs Urea & SLS

CONCLUSION

It was concluded that a simple nanoprecipitation "Bottom up" method can be successfully employed to produce ezogabine nanosuspensions. The advantage of process lies in it being totally free of organic solvents. The particle size of nanosuspension was highly dependent on parameters such as surfactant concentration and homogenization time. The process does not alter the character of bulk ezogabine and marked enhancement of dissolution rate was achieved by the reduction in particle size and by increasing the saturation solubility. The formulation F9 was found to be better when compared to other formulation in terms of particle size, saturation solubility, entrapment efficiency, and in-vitro drug release and was found to be stable at the accelerated stability conditions such as 25 ± 2 °C & 60 ± 5% RH 40 ± 2 °C and 75 ± 5% relative humidity for three months.

AUTHORS CONTRIBUTION

Conceptualization, implementation of design, generation & interpretation of data, and writing of manuscript were done by S. Revathi. Guidance, corrections & instrumental support is done by Dr. M.D. Dhanaraju

CONFLICT OF INTERESTS

Authors declare no conflict of interest.

REFERENCES

1. Shin HW, Jewells V, Hadar E, Fisher T, Hinn A. Review of Epilepsy - Etiology, Diagnostic Evaluation and Treatment. Int J Neurorehabilitation 2014; 1:130-7.

2. Orrin Devinsky, Annamaria Vezzani, Terence J. O'Brien, Nathalie Jette, Ingrid E. Scheffer, Marco de Curtis and Piero Perucca. Epilepsy. Nat Rev Dis Primers 2018; 3:1-24.

3. Judith LZ Weisenberg Michael Wong. Profile of ezogabine and its potential as an adjunctive treatment for patients with partial - onset seizures. Neuropsych Dis Treat 2011; 7:409–14

4. Pawar Anil R, Choudhari Pravin D, Ghule Prashant J, Pawar Amol R and Bankar Prakash V. Study the Effect of Surfactant Concentration and Ultrasonication Time on Aqueous Solubility, Particle Size and In-vitro Drug Diffusion of Ezogabine Nanosuspension by 3^2 Factorial Designs. Brit Med Bull 2016; 4:15–26.

5. Bhalekar MR, Upadhaya PG, Reddy S, Kshirsagar SJ, Madgulkar AR. Formulation and evaluation of acyclovir nanosuspension for enhancement of oral bioavailability. Asian J Pharm 2014; 8:110-8.

6. Eshagh Esfandi, Vahid Ramezani, Alireza Vatanara, Abdolhossein Rouholamini Najafabadi and Seyyed Pouya Hadipour Moghadda. Clarithromycin Dissolution Enhancement by preparation of Aqueous

Nanosuspensions Using Sonoprecipitation Technique. Iran J Pharm Res 2014; 13: 809-18.

7. Shetiya P, Vidyadhara S, Ramu A, Sasidhar RL, Viswanadh K. Development and characterization of a novel nanosuspension based drug delivery system of valsartan: A poorly soluble drug. Asian J Pharm 2015; 9:29-34.

8. Samar A. Afifi, Maha A. Hassan, Ali S. Abdelhameed, and Kadria A. Elkhodairy. Nanosuspension: An Emerging Trend for Bioavailability Enhancement of Etodolac. Int J Polym Sci 2015; 3:1-16.

9. Agarwal V, Bajpai M. Preparation and Optimization of Esomeprazole Nanosuspension using Evaporative Precipitation–Ultrasonication. Trop J Pharm Res 2014; 13:497-503.

10. Robert M Silverstein, Francis X Webster, David J Kiemle. Spectrometric Identification of Organic Compounds. 7th Ed. John Wiley & Sons. Inc. New York. 72 – 126.

11. Ethiraj T, Sujitha R, Ganesan V. Formulation and In-vitro Evaluation of nanosuspension of Glimepiride. Int J Pharmacy 2013; 3:875-82.

12. Sandhya J, Pavani J, Raja Reddy R. Formulation and Evaluation of Nanosuspension of Nisoldipine. Int J Pharm Sci Rev Res 2014; 24:177-81.

13. Pawar Anil R, Choudhari Pravin D, Pawar Amol R. Enhancement of Aqueous Solubility of Ezogabine: Preparation and characterization of Ezogabine nanosuspension anticipated for nose to brain targeting by 3^2 factorial design. J App Pharm 2016; 8:43-60.

14. Patel DJ, Patel JK, Pandya VM, Jivani RR, Patel RD. Optimization of formulation parameters on famotidine nanosuspension using factorial design and the desirability function. Int J Pharm Tech Res 2010; 2:155-61.

15. Bolmal UB, Manvi FV, Kotha R, Palla SS, Paladugu A, Ramamohan Reddy K. Recent advances in nanosponges as drug delivery system. Int J Pharm Sci Nanotech 2013; 6:1934– 44.

16. Borhade V, Pathak S, Sharma S, Patravale V. Formulation and characterization of atovaquone nanosuspension for improved oral delivery in the treatment of malaria. Future Med 2013.

17. Mudgil M, Pawar PK. Preparation and In Vitro/Ex Vivo Evaluation of Moxifloxacin-Loaded PLGA Nanosuspensions for Ophthalmic Application. Sci Pharm 2013; 81:591–606.

18. Chirumamilla SK, Devi U, Aravally PH, Vuppalapati L, Cherukuri S. Solubility and Dissolution Enhancement of Meropenem by Nano Suspension Approach. J Young Pharm 2017; 9:429-35.

19. Honary S, Zahir F. Effect of Zeta Potential on the Properties of Nano-Drug Delivery Systems - A Review (Part 2). Trop J Pharm Res 2013; 12:265-73.

20. Gera S, Talluri S, Rangaraj N, Sampathi S. Formulation and Evaluation of Naringenin Nanosuspensions for Bioavailability Enhancement. AAPS PharmSci Tech 2017; 18: 3151-62.

21. Devara R., Habibuddin M, Aukunuru J. Enhancement of dissolution rate of poorly soluble drug itraconazole by nanosuspension technology: its preparation and evaluation studies. Asian J Pharm Clin Res 2018; 11:414-21.

22. Kaur J, Bawa P, Yadav SR, Sharma P, Ghai D, Jyoti J, Formulation of curcumin nanosuspension using Box-Behnken design and study of impact of drying techniques on its powder characteristics. Asian J Pharm Clin Res 2017; 10:43-51.

23. Tummala S, Satish Kumar MN, Prakash A. Formulation and in vitro characterization of Carbamazepine polymeric nanoparticles with enhanced solubility and sustained release for the treatment of Epilepsy. Journal of Chemical and Pharmaceutical Research, 2015; 7(2):70-79.